Andrzej Szychowski
Structure and Environment 2023, vol. 15, (4), pp. 244-252, Article number: el 021
https://doi.org/10.30540/sae-2023-021

Structure and Environment
ISSN 2081-1500
e-ISSN 2657-6902
https://content.sciendo.com/sae
https://sae.tu.kielce.pl

sciendo

Kielce University of Technology

DOI: 10.30540/sae-2023-021

LOCAL BUCKLING OF ONE-SIDE ELASTICALLY RESTRAINED THIN-WALLED CROSS-SECTION WALL UNDER LONGITUDINAL STRESS VARIATION

WYBOCZENIE LOKALNE JEDNOSTRONNIE SPRĘŻYŚCIE ZAMOCOWANEJ ŚCIANKI PRZEKROJU CIENKOŚCIENNEGO PRZY WZDŁUŻNEJ ZMIENNOŚCI NAPRĘŻEŃ

ANDRZEJ SZYCHOWSKI*
Kielce University of Technology, Poland

Abstract

In cold-formed thin-walled cross-sections, complex phenomena, related to local and distortional buckling of slender walls containing edge fold stiffeners, occur. In order to determine the design resistance of such a cross-section in the post-buckling range, it is necessary to determine the critical stress of local buckling for individual walls. On this basis, the corresponding effective widths are determined. Subsequently, the distortional buckling effect is taken into account, typically by reducing the thickness of the substitute cross-section of the stiffener.

The paper presents approximation formulas of plate buckling coefficients (k) that are used to calculate critical local buckling stress for technically crucial stress distributions. The full range of variation of the index of elastic fixity of the longitudinal edge of the thin-walled cross-section was considered. The coefficients were determined for a more accurate, relative to Eurocode 3, computational model. Both the effect of reciprocal elastic restraint of component walls of the cross-section and the effect of longitudinal stress variation, which occurs in transversely bent beams, were taken into account.*

Keywords: thin-walled member, critical stress of local buckling, elastic restraint, longitudinal stress variation, approximation formulas

Streszczenie

W profilowanych na zimno przekrojach cienkościennych występują złożone zjawiska związane z wyboczeniem lokalnym i dystorsyjnym smukłych ścianek zawierających krawędziowe odgięcia usztywniające. W celu wyznaczenia nośności obliczeniowej takiego przekroju w zakresie nadkrytycznym należy wyznaczyć naprężenia krytyczne wyboczenia lokalnego dla poszczególnych ścianek. Na tej podstawie wyznacza się odpowiednie szerokości efektywne. W kolejnym kroku uwzględnia się efekt wyboczenia dystorsyjnego, najczęściej poprzez redukcję grubości tzw. zastępczego przekroju usztywnienia.

W pracy przedstawiono wzory aproksymacyjne płytowych współczynników wyboczeniowych (k) służące do obliczania naprężeń krytycznych wyboczenia lokalnego dla technicznie ważnych rozkładów naprężeń. Uwzględniono pełny zakres zmienności wskaźnika sprężystego utwierdzenia krawędzi podłużnej półki przekroju cienkościennego. Współczynniki*

*Corresponding Author: e-mail: aszychow@tu.kielce.pl

wyznaczono dla dokładniejszego, w stosunku do Eurokodu 3, modelu obliczeniowego. Uwzględniono zarówno efekt wzajemnego sprężystego zamocowania ścianek składowych przekroju, jak również występujący w poprzecznie zginanych belkach efekt wzdłużnej zmienności naprężeń.

Słowa kluczowe: element cienkościenny, naprężenie krytyczne wyboczenia lokalnego, sprężyste zamocowanie, wzdłużna zmienność naprężeń, wzory aproksymacyjne

1. INTRODUCTION

In thin-walled steel members with cold-formed open cross-sections containing edge fold stiffeners, there are cases of loading in which the flange (internal wall) is subjected to compression, and simultaneously, there is a longitudinal stress variation along its length. In the case of Class 4 cross-sections, local and distortional stability loss can occur, leading to a reduction in the design resistance of the cross-section in the post-buckling state. In the analysis of local buckling, these walls can be treated as thin plates loaded with normal stresses in their plane.

The most highly stressed plate elements of a bent thin-walled cross-section are usually those either two-side or one-side elastically restrained in the other plates (Fig. 1).

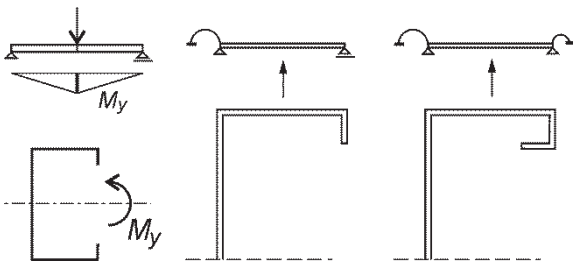

Fig. 1. Static scheme of a cold-formed thin-walled section's compressed plate (flange)

Two-side (symmetrical) restraint is found, for example, in the flanges of box sections (closed sections), where these flanges rest on webs bent in their planes. On the other hand, one-side elastic restraint against rotation is generally found in the flanges of open cold-formed cross-sections, with one side supported on the web, and the other side on the edge fold stiffeners. Depending on the type of edge fold stiffeners, either simple support of the plate (single edge fold) or elastic restraint against rotation (in the case of double or triple edge fold) can be found. From a technological point of view, single edge fold is the simplest and most cost-effective to produce, and they are quite commonly used in practice. Complex phenomena associated with local buckling and distortional buckling of slender walls and their edge fold stiffeners occur in this type of thin-walled cross-sections.

In the case of bending members with a cold-formed cross-section, the compressed flange is generally elastically restrained against rotation in the web and is also flexibly supported against deflection on the compressed edge fold. In the computational model according to [1], the wall with edge fold is treated as an internal plate rigidly supported against deflection also on this edge fold until the distortional buckling stress is reached in the cross-section. It is further assumed that the plate so separated from the cross-section is simply supported on all edges, and critical local buckling stress $\sigma_{cr,L}$ is determined for this static scheme. However, such simplification, for many technically significant geometric proportions of the cross-section, e.g., C-section or Z-section, does not correspond to the actual behavior of the thin-walled cross-section under load.

Naturally, while the assumption of simple support of the plate resting on the single edge fold (due to its low torsional stiffness further reduced by compressive stresses) should be considered appropriate, the assumption of the same simple support scheme on the web may lead to an underestimation of the critical stress $\sigma_{cr,L}$.

The correctly calculated critical stress $\sigma_{cr,L}$ (which can be determined as the product of the plate buckling coefficient k and the Euler stress σ_E) is used to determine the so-called relative plate slenderness λ_p, which is then used to determine the effective width of the compressed flange [2]. It also indirectly affects the correct determination of critical distortional buckling stress $\sigma_{cr,D}$ according to [1]. In the standard computational model, the effective width of the flange from the edge fold side is a component of the equivalent section directly affecting the value of the stress $\sigma_{cr,D}$. Once the relative slenderness λ_d (which is a function of $\sigma_{cr,D}$ and indirectly a function of $\sigma_{cr,L}$) is determined, the reduced thickness of the edge stiffener and, ultimately, the design resistance of the effective cross-section can be determined.

Therefore, the correct determination of $\sigma_{cr,L}$ according to a more accurate computational model affects both the effective widths of the compressed flange as well as indirectly the reduced thickness of the edge stiffener section and ultimately the design resistance of the entire cross-section.

The paper [3] presents the Critical Plate Method (CPM) for determining the local critical resistance (determined from the local buckling condition) and the design ultimate resistance of a thin-walled cross-section according to a more accurate, compared to Eurocode 3 standards, computational model. The local critical resistance limits in the elastic range (i.e., for $\sigma_{cr,L} < f_y$, where f_y is the design yield strength of steel) the interval of pre-buckling behavior of the cross-section, in which the assumptions of the theory of thin-walled bars by Vlasov [4] are satisfied. To effectively apply CPM, it is necessary to determine the critical stress of the weakest plate of the thin-walled cross-section, the so-called critical plate, taking into account both the effect of reciprocal elastic restraint of the walls and the effect of the longitudinal stress variation.

The purpose of this paper is to provide approximation formulas for determining the plate buckling coefficient k^* and, ultimately, the critical stress $\sigma_{cr,L}$ of an internal plate that is one side elastically restrained against rotation with the simultaneous occurrence of longitudinal stress variation. Such a plate model can be used to approximate the behavior of a compressed flange with a single edge fold (Fig. 1) of a cold-formed section under local buckling. This approach allows for a much more accurate determination of $\sigma_{cr,L}$ compared to the computational model according to [2], which ignores the influence of the elastic restraint of the walls and the longitudinal stress variation. Therefore, in case of an internal wall, the plate buckling coefficient according to [2] is $k = 4$ regardless of the degree of its elastic restraint and the longitudinal stress variation.

Approximation formulas for k^* were derived for: 1) the full range of the edge index of fixity (from hinge support through elastic restraint to complete restraint), and 2) for longitudinal stress distribution according to a linear or nonlinear function, according to a second-degree parabola.

According to the author's knowledge, such formulas are not found in technical literature.

2. CRITICAL BUCKLING STRESS

The computational model presented in the design standards for Class 4 thin-walled members [1, 2, 5] assumes that the analysis of local buckling in the cross-section can be carried out based on the concept of separating simply supported plate elements. Buckling stresses are then determined for plates separated in such a manner. In the case of the compressed internal plate considered in this paper, the buckling coefficient according to [2] is $k = 4$. After determining the relative slenderness of the individual plates (walls), the corresponding effective widths are determined, which are then combined to form the effective cross-section of the thin-walled member.

However, experimental studies of entire cross-sections e.g. [6-8], computations with the Finite Strip Method (FSM), e.g. [9, 10] or the Finite Element Method (FEM), e.g. [11], as well as theoretical analyses, e.g. [12-14], have shown that during local buckling, there is an effect of elastic interaction between rigidly connected adjacent plates (section walls). According to the author's previous papers [3, 11, 15], this effect can be can be considered in the engineering computational model.

The Critical Plate Method (CPM), presented in the paper [3] enables a more precise consideration of the real behavior of the thin-walled member compared to Eurocode 3. The study in [3] demonstrated that in many technically important cases, the local loss of stability is determined by the weakest plate ("critical plate" or "CP"), which is elastically restrained against rotation in the stronger plate ("restraining plate" or "RP").

The index of fixity along the longitudinal edge of the critical plate can be determined using formula (1):

$$\kappa = 1 / \left[\left(1 + 2D_s / \left(b_s C_\theta \right) \right) \right] \tag{1}$$

where: D_S – plate (wall s) flexural rigidity; C_θ – rotational spring stiffness of the supported edge; b_S – width of the plate.

The method of determining individual design parameters, including the procedure for iteratively determining the rotational spring stiffness C_θ, is described in detail in the paper [3].

Of course, there are cases of geometric cross-section proportions and stress distributions where the effect of elastic restraint of the component walls does not occur or is negligible and can be omitted from a technical point of view. Such cross sections were defined in the paper [3] as "zero cross-sections", along with criteria for their classification. Calculations of such cross-sections following the procedure of separating simply supported plates according to Eurocode 3 does not lead to underestimation of cross-section resistance.

In the paper [16], the issue of the loss of local stability of the compressed flange of a cold-formed cross-section (Fig. 2) was reduced to the buckling analysis of a one-side elastically restrained internal plate in the most stressed segment of the thin-walled member. The spacing of transverse stiffeners (e.g.,

ribs, diaphragms, or supports) was assumed as the length of i-th bar segment l_{si}, regardless of the spontaneously formed local buckling nodal lines [14]. Such a definition of the segment results from observations of the form of local buckling in the presence of longitudinal stress variations [8, 14]. In this case, buckling half-waves of varying length and decreasing amplitude are formed along the length of the critical plate.

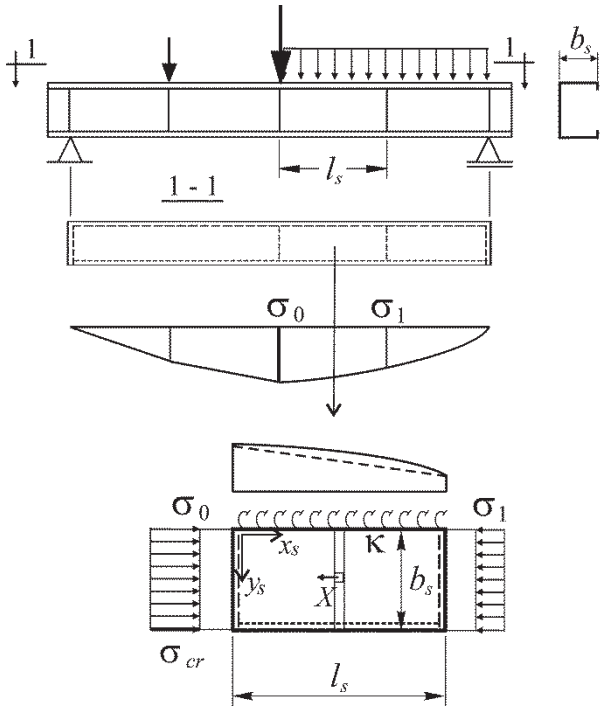

Fig. 2. Example of a compressed plate separated from a bent thin-walled member

In the case of members with cold-formed sections, the influence of the corner rounding geometry on the relevant width of the flange (wall) b_S should be taken into account. The method of determining b_S is presented in [1]. However, the influence of the corner rounding radius on the degree of elastic restraint of the wall for the most commonly used r/t_S ratios is insignificant and can be neglected. More detailed information on this subject is provided in [3].

The longitudinal variation of stresses according to a linear function or a second-degree parabola can be described using the following formulas, respectively:

$$\sigma_x = \sigma_o\left(1 - m\frac{x_s}{l_s}\right) \tag{2}$$

$$\sigma_x = \sigma_o\left(1 - m\frac{x_s^2}{l_s^2}\right) \tag{3}$$

where:

$$m = 1 - \sigma_1 / \sigma_0 \tag{4}$$

Local buckling stress ($\sigma_{cr,L}$) is referred to the most compressed edge (cf. Fig. 2) and is expressed in the form of the classical formula:

$$\sigma_{cr} = k\sigma_E \tag{5}$$

where: k – plate buckling coefficient; σ_E – Euler stress according to formula (6):

$$\sigma_E = \frac{\pi^2 E}{12\left(1-\nu^2\right)}\left(\frac{t_s}{b_s}\right)^2 \tag{6}$$

In the paper [16], the plate buckling problem was solved using the energy method. The deflection function was expressed as a polynomial-sinusoidal series. Stress variation along the length of the plate was obtained by introducing longitudinal body forces (X) according to the concept first presented in papers [17, 18]. Elastic strain energy of the plate bending and the energy of elastic restraint of the longitudinal edge ($y_S = 0$) were taken into account. The function of the work done by external forces when the plate is loaded according to equations (2) and (3) was determined from a sequence of formulas derived in the paper [19]. Based on the obtained relationships, a computer program "Ncr-plate-span-elastic(2).nb" was developed in the *Mathematica*® environment, which is used, among other things, to determine and tabulate the coefficients k. Graphs of k for elastically restrained internal plates were presented, at $\gamma_S = l_S/b_S = 1 \div 8$, for the following cases: 1) linear stress distribution for $m = 0.5$; and 2) nonlinear stress distribution for $m = 0.5$ [16].

To significantly facilitate the calculation of critical stresses for technically important combinations of parameters: $3 \le \gamma_S \le 20$; $0 \le m \le 1$; and $0 \le \kappa \le 1$, approximate formulas for plate buckling coefficients were presented in this paper, denoted by the symbol k^* for differentiation.

3. APPROXIMATION FORMULAS FOR THE COEFFICIENT k*

The approximation formulas were derived from numerical analysis of a large set of coefficient arrays obtained using the program "Ncr-plate-span-elastic(2).nb" for the following parameters: κ = 0; 0.2; 0.333; 0.429; 0.5; 0.6; 0.714; 0.8; 0.882; 0.937; 0.972; 1.0; m = 0; 0.25; 0.5; 0.75; 1; and $2 \le \gamma_S \le 20$ with a step of 0.1 (a total of 60 arrays containing

more than 10,800 coefficients). In order to increase the degree of fit of the function of plate deflection to the non-symmetric (in the longitudinal direction) form of buckling occurring with longitudinal stress variation, the parameter i_o determining the number of half-waves of the sinus function was increased from the value of 16 (for $\gamma_S \leq 8$ according to [16]) to 35 (for $\gamma_S \leq 20$).

The general form of the approximation formula for the coefficient k^*, similarly to the paper [20], is expressed by equation (7):

$$k^*(\kappa,m,\gamma) = k_\infty(\kappa) + \frac{f_q(\kappa,m)}{\gamma_S^{w_q(m)}} \tag{7}$$

where: $k_\infty(\kappa)$ – the buckling coefficient for an infinitely long and one-side elastically restrained internal plate at constant stress intensity (i.e. for $m = 0$); $w_q(m)$ – power exponent; $f_q(\kappa, m)$ – expression taking into account the longitudinal stress variation and the index of fixity according to equation (8):

$$f_q(\kappa,m) = \sum_{n=0}^{n_0}\left(\sum_{j=0}^{j_0} c_{nj} m^j\right)\kappa^n \tag{8}$$

where: c_{nj} – coefficients matrix elements determined using the least-squares method.

The buckling coefficient $k_\infty(\kappa)$ was determined as:

$$k_\infty(\kappa) = 4 + 0.452\kappa + 0.95\kappa^3 \tag{9}$$

For a linear stress distribution, the power exponent was determined as $w_q(m) = 0.68 + 0.04m$, and the calculated coefficient matrix was recorded in Table 1.

For a nonlinear stress distribution (according to a second-degree parabola), the power exponent was determined as $w_q(m) = 1.01 + 0.04m$, and the calculated coefficients matrix was recorded in Table 2.

Explicit formulas for the coefficients k^* for linear and nonlinear stress distributions were written as formulas (10) and (11), respectively, and are included in the Appendix.

Table 1. Matrix of coefficients c_{nj} for a linear stress distribution

n\j	1	2	3
0	3.689	-2.692	1.26
1	0.348	-0.343	0.18
2	0	0	0
3	0.521	-0.406	0.181

Table 2. Matrix of coefficients c_{nj} for a nonlinear stress distribution

n\j	1	2	3	4
0	3.863	-6.653	6.836	-2.603
1	0	0	0	0
2	1.135	-3.311	3.964	-1.621
3	-0.429	1.819	-2.355	0.995

In Figure 3 solid lines show the coefficient k of a one-side elastically restrained and axially compressed internal plate determined by the program according to [16], while red dashed lines show the graphs of the coefficient k^* obtained from formula (9) in the $\gamma_S = 3 \div 8$ range. The graphs were generated for a linear stress distribution according to (2) for $m = 1$ and different values of the index of fixity ($\kappa = 0 \div 1$) of the longitudinal edge ($\gamma_S = 0$). The assignment of numbers to individual curves corresponding to the index κ is given in Table 3. Dotted lines represent the classic graph of the coefficient k (the so-called garland shaped curve) for uniformly compressed and simply supported plates according to [12].

Similarly, Figure 4 compares k graphs determined according to [16] and k^* graphs calculated from formula (10) for nonlinear stress distribution according to (3) for $m = 1$.

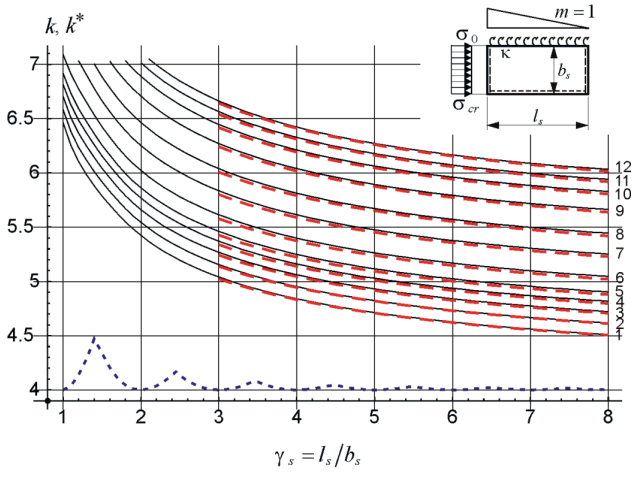

Fig. 3. Comparison of plate buckling coefficients (k, k) for linear stress distribution*

Table 3. Assignment of curve numbers in Figures 3 and 4 to the index κ

No	1	2	3	4	5	6	7	8	9	10	11	12
κ	0	0.2	0.333	0.429	0.5	0.6	0.714	0.8	0.882	0.937	0.972	1

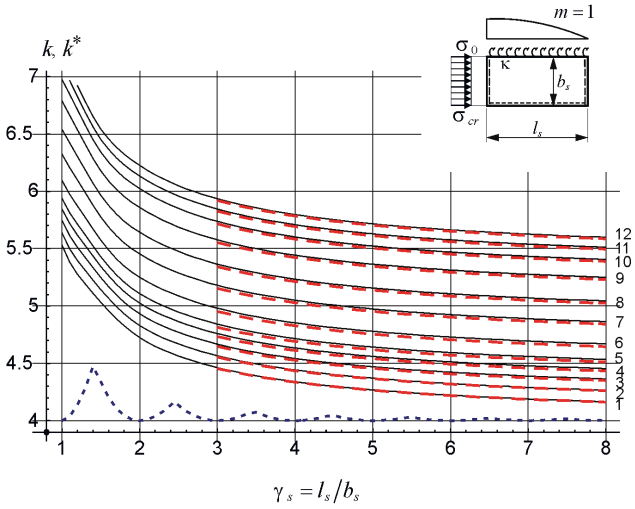

Fig. 4. Comparison of plate buckling coefficients (k, k) for nonlinear (according to the second-degree parabola) stress distribution*

A comparison of the graphs (Figs. 3 and 4) shows very good agreement between the values of the coefficients k^* according to the approximation formulas compared to the k determined by the computer program [16].

Table 4 lists the coefficients k^* for a one-side elastically restrained internal plate (for l_s/b_{s_s} = 4, 8, 12, 16) as a function of the index of fixity (κ = 0, 0.2, 0.4, 0.6, 0.8 and 1) for constant (m = 0) and linear stress distribution (m = 0.5 and 1).

From the comparison of the k^* coefficient values presented in Table 4 with the value of k = 4 according to the standard [2] it follows that: 1) taking into account only the effect of elastic restraint (i.e. for constant stress distribution, m = 0) increases k^* by a maximum of 35% (for κ = 1); 2) taking into account only the effect of longitudinal stress distribution for m = 1 (in the absence of elastic restraint, i.e. for κ = 0) causes an increase in k^* from 20.8% for l_s/b_s = 4 to 7.8% for l_s/b_s = 16; 3) taking into account the total impact of the above-mentioned effects increases k^* from 60.3% for l_s/b_s = 4, κ = 1 and m = 1 to 44.3% for l_s/b_s = 16, κ = 1 and m = 1.

Similarly, Table 5 provides the coefficients k^* for the nonlinear (according to the second-degree parabola) stress distribution (m = 0.5 and 1). Note: to facilitate comparisons, Table 5 also includes values for m = 0 (i.e. a constant stress distribution along the entire length).

From the comparison of the k^* coefficient values presented in Table 5 with the value of k = 4 according to the standard [2] it follows that: 1) taking into account only the effect of elastic restraint (i.e. for constant stress distribution, m = 0) increases k^* (similarly to Table 4) by a maximum of 35% (for κ = 1); 2) taking into account only the effect of longitudinal stress distribution for m = 1 (in the absence of elastic restraint, i.e. for κ = 0) causes an increase in k^* from 8.5% for l_s/b_s = 4 to 2% for l_s/b_s = 16; 3) taking into account the total impact of the above-mentioned effects increases k^* from 44.5% for l_s/b_s = 4, κ = 1 and m = 1 to 37.3% for l_s/b_s = 16, κ = 1 and m = 1.

A comparison of the graphs shown in Figure 3 and Figure 4 and a comparison of the values in Table 4 and

Table 4. Coefficients k for the linear stress distribution as a function of index κ*

l_s/b_s	m	κ					
		0	0.2	0.4	0.6	0.8	1
4	0	4	4.10	4.24	4.48	4.85	5.40
	0.5	4.50	4.61	4.77	5.02	5.42	6.01
	1	4.83	4.94	5.11	5.37	5.79	6.41
8	0	4	4.10	4.24	4.48	4.85	5.40
	0.5	4.31	4.41	4.56	4.81	5.20	5.78
	1	4.51	4.61	4.77	5.02	5.42	6.01
12	0	4	4.10	4.24	4.48	4.85	5.40
	0.5	4.23	4.34	4.48	4.73	5.11	5.69
	1	4.38	4.48	4.63	4.88	5.28	5.86
16	0	4	4.10	4.24	4.48	4.85	5.40
	0.5	4.19	4.29	4.44	4.68	5.06	5.63
	1	4.31	4.41	4.56	4.81	5.20	5.77

Table 5. Coefficients k^* for the nonlinear (according to the second-degree parabola) stress distribution as a function of index κ

l_s/b_s	m	κ					
		0	0.2	0.4	0.6	0.8	1
4	0	4	4.10	4.24	4.48	4.85	5.40
	0.5	4.23	4.33	4.48	4.72	5.10	5.67
	1	4.34	4.44	5.58	4.83	5.21	5.78
8	0	4	4.10	4.24	4.48	4.85	5.40
	0.5	4.11	4.21	4.36	4.60	4.97	5.53
	1	4.16	4.26	4.41	4.65	5.02	5.59
12	0	4	4.10	4.24	4.48	4.85	5.40
	0.5	4.07	4.17	4.32	4.55	4.93	5.49
	1	4.11	4.20	4.35	4.59	4.96	5.52
16	0	4	4.10	4.24	4.48	4.85	5.40
	0.5	4.05	4.15	4.30	4.53	4.91	5.47
	1	4.08	4.18	4.32	4.56	4.93	5.49

Table 5 show that: 1) with an increase in the index κ and the parameter m, the values of the plate buckling coefficients (k, k^*) increase, 2) with an increase in plate length, the favorable effect of longitudinal stress variation decreases, but the favorable effect of elastic restraint remains, 3) smaller values of k and k^* for the same values of parameters (κ, m, γ_S) were obtained for nonlinear stress distribution.

Based on numerous computational tests (performed also for intermediate values of parameters m and κ), it was found that a safe (slightly conservative) estimate of the coefficient k^* can be obtained from formulas (9) and (10) in the following ranges: $3 \le \gamma_S \le 20$; $0 \le m \le 1$; $0 \le \kappa \le 1$. For very long plates ($\gamma_S > 20$), for $0 \le \kappa \le 1$, a conservative estimate of the coefficient k^* can be obtained directly from formula (9).

4. SUMMARY

Enhancing the accuracy of representing the behavior of thin-walled members, such as cold-formed ones, in engineering computational models is a natural direction in the development of modern design methods. Currently, there is an increased interest in approximation formulas which would take into account more advanced computational models of steel elements, e.g. [21, 22].

Taking into account both the index of fixity ($0 \le \kappa \le 1$) and longitudinal stress variation ($0 \le m \le 1$) in calculations of thin-walled members leads to a more accurate assessment of critical stress in relation to the computational model according to [2]. The standard model ignores the above-mentioned effects, which in many technically important cases leads to underestimation of $\sigma_{cr,L}$.

The approximation formulas for the plate buckling coefficient k^* provided in this paper allow for a relatively straightforward determination of critical stress in compressed and one-side elastically restrained internal walls with longitudinal stress variation. Such a plate-load system can model the behavior of the compression flange of a thin-walled section subjected to bending.

Correct determination of the elastic critical stress of local buckling under loading that induces longitudinal stress variation determines the interval of pre-buckling behavior of a thin-walled member [8, 14] and limits the validity interval of Vlasov's theory [4] in the elastic range ($\sigma_{cr,L} \le f_y$). Critical stress determined in this way serve for a more precise calculation of the relative slenderness of the critical plate and the assessment of the design resistance of the cross-section based on the CPM [3].

APPENDIX

Approximation formulas for plate buckling coefficients k^*:

1) linear stress distribution:

$$k^*(\kappa,m,\gamma) = 4 + 0.452\kappa + 0.95\kappa^3 + \Big[3.689m - 2.692m^2 + 1.26m^3 + \Big(0.348m - 0.343m^2 + 0.18m^3\Big)\kappa + \\ + \Big(0.521m - 0.406m^2 + 0.181m^3\Big)\kappa^3\Big] / \gamma_s^{(0.68+0.04m)} \tag{10}$$

2) non-linear stress distribution (according to the second-degree parabola):

$$k^*(\kappa,m,\gamma)=4+0.452\kappa+0.95\kappa^3+\Big[3.863m-6.653m^2+6.836m^3-2.603m^4+$$
$$+\left(1.135m-3.311m^2+3.964m^3-1.621m^4\right)\kappa^2+ \tag{11}$$
$$+\left(-0.429m+1.819m^2-2.355m^3+0.995m^4\right)\kappa^3\Big]/\gamma_s^{(1.01+0.04m)}$$

References

[1] EN 1993-1-3:2006 Eurocode 3 – Design of steel structures – Part 1-3: General rules – Supplementary rules for cold-formed members and sheeting.

[2] EN 1993-1-5:2006 Eurocode 3 – Design of steel structures – Part 1-5: Plated structural elements.

[3] Szychowski A.: *Computation of thin-walled cross-section resistance to local buckling with the use of the Critical Plate Method. Archives of Civil Engineering*, 2016, Vol. 62, Issue 2, 229-264; doi:10.1515/ace-2015-0077.

[4] Vlasov V.Z.: *Thin-Walled Elastic Beams*. Israel Program for Scientific Translations, Jerusalem, 1961.

[5] EN 1993-1-1:2006 Eurocode 3 – Design of steel structures – Part 1-1: General rules and rules for buildings.

[6] Beale R.G., Godley M.H.R, Enjily V.: *A theoretical and experimental investigation into cold-formed channel sections in bending with the unstiffened flanges in compression*. Computer & Structures 79, 2001, 2403-2411, doi.org/10.1016/S0045-7949(01)00073-6.

[7] Kotełko M., Lim T.H., Rhodes J.: *Post – failure behaviour of box section beams under pure bending (an experimental study)*. Thin-Walled Structures 38, (2000), 179-194, doi.org/10.1016/S0263-8231(00)00032-X.

[8] Kowal Z., Szychowski A.: *Experimental determination of critical loads in thin-walled bars with Z-section subjected to warping torsion*. Thin-Walled Structures 75, 2014, 87-102, doi.org/10.1016/j.tws.2013.10.020.

[9] Papangelis J.P., Hancock G.J.: *Computer analysis of thin-walled structural members*, Computer & Structures Vol. 56. No. 1. 1995, 157-176, doi.org/10.1016/0045-7949(94)00545-E.

[10] Schafer B.W., Ádány S.: *Buckling analysis of cold-formed steel members using CUFSM: conventional and constrained finite strip methods*. Proceedings of the Eighteenth International Specialty Conference on Cold-Formed Steel Structures, Orlando, FL. October 2006.

[11] Szychowski A., Brzezińska K.: *Local buckling and resistance of continuous steel beams with thin-walled I-shaped cross-sections*. Applied Sciences, 2020, 10(13), 4461, doi:10.3390/app10134461.

[12] Bulson P.S.: *The Stability of Flat Plates*, Chatto and Windus, London 1970.

[13] Jakubowski S.: *Buckling of thin-walled girders under compound loa*d. Thin-Walled Structures 1988, 6,129-150, doi.org/10.1016/0263-8231(88)90004-3.

[14] Szychowski A.: *A theoretical analysis of the local buckling in thin-walled bars with open cross-section subjected to warping torsion*. Thin-Walled Structures 76 (2014) 42-55, doi.org/10.1016/j.tws.2013.11.002.

[15] Brzezińska K., Szychowski A.: *Stability and resistance of steel continuous beams with thin-walled box sections*. Archives of Civil Engineering, 2018, Vol. 64, Issue 4, 123-143; doi.org/10.2478/ace-2018-0048.

[16] Szychowski A.: *Local stability of the compressed flange of a cold-formed thin-walled section* (in Polish). Zeszyty Naukowe Politechniki Rzeszowskiej Nr 276, Seria: Budownictwo i Inżynieria Środowiska, Zeszyt 58, Nr 3/2011/II, 307-314.

[17] Kowal Z.: *The stability of compressed flange of plate girder with a box section* (in Polish). Zeszyty Naukowe Politechniki Wrocławskiej, Budownictwo 1965, 122, 73-85.

[18] Kowal Z.: *The stability top metal plate of pontoon foundation* (in Polish). Węgiel Brunatny 1966; 4: 331-333.

[19] Szychowski A.: *The stability of eccentrically compressed thin plates with a longitudinal free edge and with stress variation in the longitudinal direction*. Thin-Walled Structures 2008; 46 (5): 494-505, doi.org/10.1016/j.tws.2007.10.009.

[20] Szychowski A.: *Stability of cantilever walls of steel thin-walled bars with open cross-section*. Thin-Walled Structures 94 (2015), 348-358, doi.org/10.1016/j.tws. 2015.04.029.

[21] Gardner L., Fieber A., Macorini L.: *Formulae for calculating elastic local buckling stresses of full structural cross-sections*. Structures 17 (2019): 2-20, doi.org/10.1016/j.istruc.2019.01.012.

[22] Piotrowski R., Szychowski A.: *Impact of support closed section ribs on the critical moment for lateral torsional buckling of steel beams*. Structure and Environment, vol. 10, no. 1, pp. 5-18, 2018, doi: 10.30540/sae-2018-001.

Acknowledgements

Internal scientific research financed from the research subsidy entitled: “Stability and resistance of steel compression and bending members under local and overall (internode) buckling”, No. 02.0.18.00/1.02.001, SUBB. BKWK. 23.002.